JOURNAL OF CATALYSIS 146, 69–81 (1994)

Deactivation Model with Residual Activity to Study Thioresistance and Thiotolerance of Naphtha Reforming Catalysts

A. Borgna, T. F. Garetto, A. Monzón,* and C. R. Apesteguía[1]

*Instituto de Investigaciones en Catálisis y Petroquímica-INCAPE- (UNL-CONICET), Santiago del Estero 2654, 3000-Santa Fe, Argentina, and * Departamento de Ingeniería Química, Universidad de Zaragoza, 50009 Zaragoza, Spain*

Received June 17, 1993; revised September 13, 1993

The relative sensitivity to sulfur poisoning of typical commercially employed naphtha reforming catalysts was studied using a cyclohexane dehydrogenation as test reaction and thiophene as the poisoning molecule. Monometallic Pt/Al_2O_3 and bimetallic $Pt–Re/Al_2O_3$, $Pt–Ir/Al_2O_3$, $Pt–Ge/Al_2O_3$, and $Pt–Sn/Al_2O_3$ catalysts were used. A deactivation model with residual activity (DMRA) was employed for determining both the thiotolerance and the thioresistance of the catalysts. The DMRA model was developed by using Langmuir–Hinshelwood kinetics and assuming the rate-determining step in the poisoning mechanism to be reversible. The thiotolerance was in the order Pt–Ge > Pt–Ir ≅ Pt ≅ Pt–Sn > Pt–Re. According to DMRA equations, the thiotolerance decreases when K_s, the adsorption equilibrium constant of H_2S on the catalysts, increases. This DMRA model prediction was verified by measuring the quantities of total and irreversibly held sulfur following exposure of the catalysts to H_2/H_2S mixtures. The thioresistance decreased in the sequence Pt–Ge > Pt–Ir ≅ Pt > Pt–Re > Pt–Sn. From DMRA equations it was established that the thioresistance is primarily a function of k_p, the reaction rate constant for the hydrogenolysis of adsorbed thiophene; the higher the k_p value, the lower the catalyst thioresistance. Bimetallic $Pt–Ge/Al_2O_3$ was the most thioresistant and thiotolerant catalyst. This superior performance is explained by assuming that upon reduction at 773 K a fraction of the Ge cations is reduced and forms bimetallic Pt–Ge particles. The formation of Pt–Ge clusters increases the electrophilic character of platinum, thereby weakening the strength of the S–Pt bond and reducing the amount of irreversibly held sulfur on platinum.

INTRODUCTION

Sulfur poisoning of Pt-based catalysts employed in naphtha reforming has been an important subject of fundamental and applied research since the late 1950s, when pioneer studies using monometallic Pt/Al_2O_3 catalysts were published (1–3). The introduction in the late 1960s of bimetallic catalysts exhibiting superior activity and selectivity drastically improved the naphtha reforming process (4). However, certain bimetallic catalysts such as $Pt–Re/Al_2O_3$ catalysts, are substantially more sensitive to sulfur poisoning than monometallic Pt catalysts. For example, new "skewed" catalysts containing Re/Pt atomic ratio higher than 1 admit a maximum sulfur level of 0.5 ppm in the feed (5).

Bimetallic catalysts most often used in conventional naphtha reforming process consisting of three or four consecutive fixed-bed reactors are Pt–Re and Pt–Ir catalysts. Bimetallic Pt–Sn and Pt–Ge catalysts have also been occasionally employed. Consequently, sulfur poisoning has been mostly performed on monometallic Pt/Al_2O_3 or bimetallic $Pt–Re/Al_2O_3$ and $Pt–Ir/Al_2O_3$ reforming catalysts (6–8). To date no studies have appeared in the open literature on sulfur poisoning of $Pt–Ge/Al_2O_3$ or $Pt–Sn/Al_2O_3$ in spite of the fact that Pt–Ge and Pt–Sn catalysts are good candidates for use in low-pressure naphtha reforming processes employing continuous catalyst regeneration (CCR). Since CCR processes require catalysts which do not need complex activation procedures, bimetallic Pt–Sn and Pt–Ge catalysts are receiving renewed attention (9). It is therefore of both fundamental and practical interest to undertake studies of sulfur poisoning of Pt–Ge and Pt–Sn catalysts.

Although several reviews have recently been published (10, 11), our understanding of the mechanism of sulfur poisoning of metallic catalysts under industrial conditions is lacking. Knowledge regarding the sulfur resistance of bimetallic catalysts is especially lacking. Other than the inherent complexity of poisoning in bimetallic systems, there are a number of reasons related to the method employed to characterize sulfur resistance that further complicate the analysis of sulfur deactivation. Some of these reasons are, in our opinion, the following:

(i) How the "sensitivity" to sulfur poisoning is defined. A number of deactivation parameters such as: initial deactivation (12), toxicity (13), normalized initial deactivation (14), steady-state activity (15), deactivation functions (16), and deactivation constants of pseudo homogeneous

[1] To whom correspondence should be addressed.

0021-9517/94 $6.00

kinetics (17), have been indistinctly used to characterize and compare the sensitivity to sulfur poisoning of different catalysts. However, information gained using these different parameters is not necessarily the same; thus, conclusions may be different depending on the deactivation parameter used.

(ii) How the deactivation parameters are obtained from experimental data. Most authors derive the parameters either directly from experimental curves (typically, the initial slope of the plots of activity against time) or from mathematical functions which approximate the actual deactivation law. It is often preferable to obtain the deactivation parameters from a deactivation equation derived by modelling active sites balances coupled to deactivation mechanisms. The general approach based on Langmuir–Hinshelwood kinetics with non-separable variables (18–20) gives more insight into the poisoning mechanism.

(iii) How simultaneous deactivation processes are taken into account. Sulfur poisoning of metallic catalysts often takes place in presence of simultaneous deactivation by coking or metal sintering. However, few studies have been undertaken to discern the influence of these simultaneous deactivation processes on the sulfur poisoning mechanism (21, 22). It has previously been shown that the coadsorption of a reactant on platinum may change both the sulfur poisoning mechanism and the thermodynamics of sulfur adsorption (23–25).

The aim of the present study is to establish the relative sensitivity to sulfur poisoning of naphtha reforming catalysts currently used by industry, namely alumina-supported Pt, Pt–Re, Pt–Ir, Pt–Ge, and Pt–Sn catalysts. Initially, fundamental studies dealing with the characteristics of the sulfur adsorption on Pt-based catalysts were performed (26–29). Then a general investigation of the kinetics and mechanism of sulfur poisoning was undertaken using a deactivation model with Langmuir–Hinshelwood-type kinetics and nonseparable variables. Benzene hydrogenation, a monofunctional metallic reaction, was used to ascertain the effect of sulfur poisoning of Pt, Pt–Re, and Pt–Ir catalysts in presence of simultaneous coke deactivation (22).

In the present paper we have extended the above studies to include Pt–Ge and Pt–Sn catalysts. Cyclohexane dehydrogenation was employed as reaction test and thiophene as poisoning molecule. Coke deactivation was negligible under the experimental conditions used. We have developed a deactivation model with residual activity by using Langmuir–Hinshelwood kinetics and by assuming that the rate-determining poisoning step is reversible. Special emphasis was given to defining and calculating both thioresistance and thiotolerance deactivation parameters required to establish the relative sulfur sensitivies of the catalysts investigated.

EXPERIMENTAL

Monometallic Pt catalyst was made by impregnation at 303 K of a high-purity γ-Al_2O_3 powder (Cyanamid Ketjen CK300) with an aqueous solution of chloroplatinic acid and HCl. The CK300 alumina has BET surface area of 180 m^2/g, pore volume of 0.49 cm^3/g and contains 50 ppm sulfur. After impregnation, the sample was dried 12 h at 393 K and heated in air stream to 773 K. Then the chlorine content was regulated using a gaseous mixture of HCl, water and air. Finally, the sample was purged with N_2 and reduced in flowing H_2 for 8 h at 773 K. Bimetallic Pt–Sn catalyst was prepared by coimpregnation of alumina CK300 with aqueous solution of Cl_2Sn, H_2PtCl_6 and HCl. Coimpregnation was carried out at 303 K and the volume of the impregnating solution was 0.7 ml/g support. After drying overnight at 393 K the sample was calcined in air for 5 h at 773 K, purged in N_2 and reduced in flowing H_2 at the same temperature. The Pt–Ir catalyst was prepared using the wet impregnation method. Alumina CK300 was impregnated with an aqueous solution containing H_2PtCl_6, $(NH_4)_2IrCl_6$, and HCl. After evaporation of water, the sample was dried 12 h at 393 K and heated in air to 773 K. Finally, the sample was submitted to the same procedures of chlorine regulation and H_2 reduction described above for monometallic Pt/Al_2O_3 catalyst. Bimetallic $Pt–Re/Al_2O_3$ (Cyanamid Ketjen CK433) and $Pt–Ge/Al_2O_3$ (Union Oil Products, UOP R22) catalysts were obtained from commercial sources. The sulfur content of these two catalysts was <80 ppm. The chlorine and metal loadings of all the Pt-based catalysts are given in Table 1. Additionally, three control samples which did not contain platinum were prepared. The samples were supported on alumina CK300 and contained, respectively, Ge, Sn, and Re. The Ge(0.3 wt%)/Al_2O_3 and Sn(0.3 wt%)/Al_2O_3 samples were prepared by impregnation of alumina at 303 K with hydrochloric solutions of $GeCl_4$ and $SnCl_2$, respectively. Monometallic Re(0.55%)/Al_2O_3 sample was made by impregnating alumina powder with an aqueous solution of perrhenic acid. After impregnation the three reference samples were dried, calcined, and reduced following the same procedure described above for the preparation of the monometallic Pt/Al_2O_3 catalyst.

Accessible metal fractions were determined by chemisorption of hydrogen (HC), oxygen (OC), and carbon monoxide (CO). The volumetric adsorption experiments were performed at room temperature in a conventional vacuum apparatus equipped with an MKS Baratron pressure gauge. In the case of H_2 and CO chemisorption the double isotherm method was used (30): the first isotherm gave the total gas uptake and the second, obtained after 1 h of evacuation at room temperature, the weakly adsorbed gas. By difference, the amount of strongly adsorbed gas was determined. The pressure range was 0–50 Torr (1

TABLE 1

Main Characteristics of the catalysts used in this work.

Catalysts	Metal loading (%)	Cl (%)	Accessible metal fraction (%)	$(-r_A)_0$[a]	N[b] × 10^{-3}
Pt	0.53 Pt	0.95	67	57.7	16.8
Pt–Re	0.30 Pt–0.30 Re	0.78	51[c]	36.0[c]	13.5[c]
Pt–Ir	0.30 Pt–0.05 Ir	0.83	58[c]	33.5[c]	11.3[c]
Pt–Ge	0.35 Pt–0.24 Ge	0.81	10[d]	1.4[d]	2.7[d]
Pt–Sn	0.26 Pt–0.30 Sn	0.90	51[d]	5.7[d]	2.2[d]

Note. All the catalysts were supported on alumina.

[a] Reaction rate in moles of cyclohexane/h · g metal.

[b] Turnover number, in h^{-1}

[c] Values calculated by considering the total metal loading.

[d] Values calculated by considering only the Pt loading.

Torr = 133.32 Pa) and extrapolation to zero pressure was used as a measure of the gas uptake on the metal. Samples were reduced with H_2 for 2 h at 773 K prior to performing gas chemisorption experiments.

Sulfur adsorption experiments were carried out in a flow reactor at 773 K and atmospheric pressure using a gaseous mixture containing 50 ppm of H_2S in H_2. The evolution of H_2S was measured by frontal analysis with a photo-ionization detector. Samples (100 mg) were reduced in H_2 for 2 h at 773 K and then the H_2S/H_2 mixture was admitted to the reactor. The total amount of adsorbed sulfur was determined when the sample was saturated by H_2S and a constant concentration of H_2S in the exit gas was observed. Then, the sample was treated with pure H_2 at the same temperature and the amount of reversibly held sulfur was determined. The amount of irreversibly held sulfur was calculated as the difference between total and reversibly adsorbed sulfur.

Cyclohexane dehydrogenation was carried out at atmospheric pressure in a fixed-bed reactor. The reactant was delivered to the reactor with a motor-driven syringe and was vaporized in a preheating section. Prior to passage down through the catalyst bed, the reactant was brought to reaction temperature in admixture with hydrogen. Hydrogen was passed through Deoxo and molecular sieve drying units. The catalyst bed temperature was controlled to within 1 K. On-line chromatographic analysis were performed using a gas chromatograph equipped with a flame ionization detector. The reaction was performed at 573 K and the cyclohexane and hydrogen pressures were maintained constants (P_H = 0.977 atm; P_C = 0.023 atm; 1 atm = 101.325 kPa). The feed was doped with thiophene in concentrations between 0–10 ppm of S. The initial conversion was always less than 10% and care was taken to minimize diffusional limitations. Catalyst extrudates were crushed to 40–80 mesh fraction. Cyclohexane and benzene were the only products detected. Catalysts were reduced *in situ* with flowing H_2 for 2 h at 773 K before performing the catalytic tests.

RESULTS

I. Catalyst Characterization

I.1. Gas chemisorption. The accessible metal fractions of the catalysts were determined by selective gas chemisorption. In the case of Pt, Pt–Ir, and Pt–Re catalysts there is a general agreement in the literature pertaining to the most suitable methods for estimating the respective metallic dispersions. We have used hydrogen chemisorption (HC) and assumed a stoichiometry $H/Pt_s = 1$, where Pt_s implies Pt atom on surface, to measure the dispersion of monometallic Pt/Al_2O_3 catalyst. The same method was employed to calculate the total (Pt + Ir) dispersion of Pt–Ir catalyst (6). Total (Pt + Re) dispersion of Pt–Re catalyst was obtained by using oxygen chemisorption (OC) and stoichiometries $O/Pt_s = O/Re_s = 1$ (31).

In contrast to the above materials, there is little information addressing the determination of the accessible Pt fraction in Pt–Ge and Pt–Sn catalysts by gas chemisorption (32–35). The main difficulty in developing a standard method arises from the fact that both catalysts are able to form bimetallic clusters or alloys and that the extent of alloying depends on the preparation method and on the reduction treatment employed. It is well known that alloying can drastically change the chemisorption capacity of the active metal (36), thus one can expect that the values obtained by using any gas chemisorption method will be strongly dependent on the previous preparation and activation procedures. We have used OC and HC to characterize Pt–Sn catalysts. The Pt dispersion was 51 and 35% using OC and HC, respectively. Since it has been reported (32) that H_2 chemisorption is not suitable for measuring the Pt dispersion of $Pt–Sn/Al_2O_3$ catalysts

we have included in Table 1 the value of the accessible Pt fraction obtained by employing O_2 chemisorption.

In previous studies (34, 35) hydrogen chemisorption was used for selectively measuring the Pt dispersion in Pt–Ge catalysts. In this paper, the accessible Pt fraction of bimetallic Pt–Ge catalyst was measured by using HC, OC, and CO. For this particular catalyst we used two different reduction temperatures, 573 and 773 K, before performing gas chemisorption measurements. We found that the values of the metallic dispersion were strongly dependent on the reduction temperature. When reduction was performed at 573 K, Pt dispersion measured using the three methods was similar; the values were D_{HC} = 53%, D_{OC} = 49%, and D_{CO} = 54%. When a reduction treatment of 773 K was used the values of Pt dispersion were not coincident; in fact, we obtained D_{HC} = 10%, D_{OC} = 48%, and D_{CO} = 36%. Taking into account that the standard activation procedure of the catalysts prior to activity testing consisted of reduction with H_2 at 773 K, we included in Table 1 the value of Pt dispersion calculated by hydrogen chemisorption after similar reduction pretreatment of the catalyst at 773 K, i.e., D_{Pt} = 10%.

I.2. Catalyst activity without S poisoning. In order to measure the catalytic activity of fresh catalysts pure cyclohexane without thiophene doping was used as reactant. In all the cases, the deactivation by coke formation was negligible. The values of the specific reaction rates, $(-r_A)_0$, and of the turnover numbers, N, are presented in Table 1. Monometallic Pt and bimetallic Pt–Re and Pt–Ir catalysts exhibited similar dehydrogenation activities. In agreement with others (37, 38) we found that the addition of Ge or Sn drastically diminishes the activity of Pt. As it is shown in Table 1, the $(-r_A)_0$ values corresponding to Pt–Ge or Pt–Sn catalysts were about one order of magnitude lower than those obtained for Pt, Pt–Re, or Pt–Ir catalysts.

II. Sulfur Adsorption Experiments

The adsorption of sulfur on Pt-based catalysts takes place on both the metal and the support (27). Part of the adsorbed sulfur is resistant to hydrogen treatment at 773 K (S_i, irreversibly held sulfur) and is located on the metal. The other part of the adsorbed sulfur is eliminated in hydrogen at 773 K (S_r, reversibly held sulfur) and is probably located on both metal and support sites. Table 2 shows the amounts of sulfur adsorbed on the Pt-based catalysts and on the three reference samples which did not contain platinum. The amounts of the total (S_t) and irreversibly adsorbed sulfur on monometallic Pt/Al_2O_3 catalyst were S_t/Pt_s = 0.87 and S_i/Pt_s = 0.38, respectively. These values are in good agreement with the corresponding atomic ratios reported in previous studies on similar catalysts by using microgravimetric techniques (39). The number of sulfur atoms that bimetallic Pt–Ir/Al_2O_3 catalyst adsorbed per surface metal atom were close to those adsorbed by the monometallic Pt catalyst. Somewhat higher sulfur adsorption was found for the bimetallic Pt–Re/Al_2O_3 catalyst (S_t/Me_s = 1.21; S_i/Me_s = 0.65); this results from a higher capacity for adsorbing sulfur by Re than Pt, as can be inferred from Table 2 where the amounts of sulfur adsorbed on Re/Al_2O_3 and Pt/Al_2O_3 samples are compared. Regarding the bimetallic Pt–Ge catalyst, it is worth noting that the amount of sulfur irreversibly held on this catalyst and on Ge/Al_2O_3 sample is negligible. Germanium appears to weaken the strength of the sulfur–platinum bond thereby reducing the amount of irreversibly held sulfur on platinum. Finally, the S_i adsorption on Sn/Al_2O_3 sample was also negligible; however, the presence of tin did not diminish to a significant extent the S_i adsorption on platinum in bimetallic Pt–Sn/Al_2O_3. In fact, the ratio S_i/Pt_s was 0.30 in the Pt–Sn/Al_2O_3 catalyst compared to the value of 0.38 determined for monometallic Pt/Al_2O_3 catalyst.

III. Catalytic Tests with Sulfur Poisoning

III.1 Deactivation model with residual activity. Figure 1 illustrates the time-on-stream behavior of the Pt–Sn catalyst during the dehydrogenation of the cyclohexane feed both with and without added thiophene. Similar curves representing the activity decay as a function of time were obtained for the other catalysts. The activity is defined as $a = (-r_A)_t/(-r_A)_0$, where $(-r_A)_0$ and $(-r_A)_t$ are the reaction rates at zero time and at time t, respectively. The deactivation curves reached steady-state values, a_{ss}, different from zero. This behavior can not be represented by using linear, exponential or hyperbolic functions which are obtained when pseudohomogeneous deactivation kinetics like $-(da/dt) = k_d P_T^n a^d$ with d equal to 0, 1, or 2, respectively, are used (40). As an example, we have represented in Fig. 2 the fitting obtained when an exponential function is used. It is clear that the high-time points deviate from the straight line in the (ln a)-vs-time plot.

Deactivation processes showing residual activity have been studied by employing two different approaches. Fuentes (41) used empirical equations like $-(da/dt) = Q_{(P,T)}(a-a_{ss})^d$ or $-(da/dt) = Q_{(P,T)}(a^d-a_{ss}^d)$, where $Q_{(P,T)}$ represents a global kinetic term, to account for the asymptotic behavior of the deactivation curves. Corella *et al.* (21) employed Langmuir-Hinshelwood kinetics to analyze different deactivation processes leading to the retention of a residual activity. In this paper we develop a deactivation model with residual activity (DMRA) which relates the disappearance rate of active sites to a reversible reaction in the controlling step of sulfur poisoning. The following elementary steps for cyclohexane dehydrogenation (42)

TABLE 2

Sulfur Adsorption Experiments

Sample	S_t, total S		S_r, reversible S		S_i, irreversible S	
	μmol/g cat	S_t/Me_s[a]	μmol/g cat	S_r/Me_s[a]	μmol/g cat	S/Me_s[a]
Pt	15.94	0.87	8.96	0.49	6.98	0.38
Pt–Re	19.42	1.21[b]	8.97	0.56[b]	10.45	0.65[b]
Pt–Ir	8.55	0.82[b]	4.28	0.41[b]	4.27	0.41[b]
Pt–Ge	1.37	0.77[c]	1.33	0.75[c]	0.04	0.02[c]
Pt–Sn	4.15	0.61[c]	2.11	0.31[c]	2.04	0.30[c]
Re	32.21	—	5.64	—	26.57	—
Ge	4.15	—	4.30	—	0.0	—
Sn	4.65	—	4.65	—	0.0	—

Note. Mixture: H_2S/H_2, 50 ppm H_2S; T = 773 K; P = 1 atm. All the samples were supported on alumina.

[a] Atoms of sulfur adsorbed per surface metal atom.

[b] Values calculated by considering the total metal loading.

[c] Values calculated by considering only the Pt loading.

and thiophene poisoning (43) are considered. The nomenclature used is given in the Appendix.

Cyclohexane dehydrogenation:

$$C_6H_{12} + L \rightleftharpoons C_6H_{10} \cdot L + H_2 \qquad K_I = P_H C_{CL}/P_C C_L$$
$$C_6H_{10} \cdot L \rightleftharpoons C_6H_8 \cdot L + H_2 \qquad k_c, k_c'$$
$$C_6H_8 \cdot L \rightleftharpoons C_6H_6 \cdot L + H_2 \qquad K_{II} = C_{BL}P_H/C_{BHL}$$
$$C_6H_6 \cdot L \rightleftharpoons C_6H_6 + L \qquad K_B = C_{BL}/P_B C_L.$$

Thiophene poisoning:

$$\text{Thiophene} + L \rightleftharpoons \text{Thiophene} \cdot L \qquad K_T = C_{TL}/P_T C_L$$
$$\text{Thiophene} \cdot L + 3H_2 \rightleftharpoons \text{Butane} + S \cdot L \qquad k_p, k_p'$$
$$S \cdot L + H_2 \rightleftharpoons H_2S + L \qquad K_S = P_H C_{SL}/P_S C_L$$

The rate-determining step of the poisoning mechanism is the reversible reaction that represents the hydrogenolysis of the adsorbed thiophene. Hence, the rate of appearance of poisoned sites is

$$dC_{SL}/dt = k_p K_T P_H^3 P_T C_L - k_p' P_{but} C_{SL}. \qquad [1]$$

By a balance of active sites on the catalyst surface at time t, it follows that

$$C_L = (L_0 - C_{SL})/(1 + K_T P_T + \Sigma K_i P_i), \qquad [2]$$

where,

$$\Sigma K_i P_i = K_I P_C/P_H + P_H K_B P_B/K_{II} + K_B P_B.$$

When Langmuir–Hinshelwood kinetics is employed, it is well known (20) that from the definition of activity one obtains

$$a = (L_0 - h C_{SL})^m/L_0^m, \qquad [3]$$

where m and h are the number of active sites involved in the controlling step of the main and deactivation reactions, respectively. In our case, $m = h = 1$ and Eq. [3] becomes

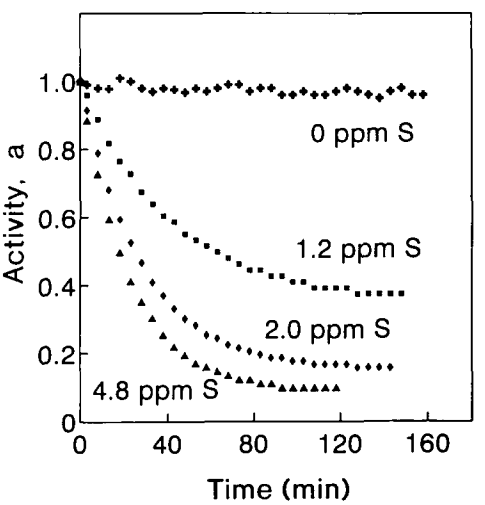

FIG. 1. Cyclohexane dehydrogenation activity (a) as a function of time and feed sulfur concentration over the bimetallic Pt–Sn catalyst; 1.2–4.8 ppm sulfur feeds obtained by thiophene addition.

$$a = \frac{(L_0 - C_{SL})}{L_0} = \frac{(1 + K_T P_T + \Sigma K_i P_i) C_L}{L_0}. \quad [4]$$

From Eqs. [4] and [1], we obtain

$$-(da/dt) = \frac{k_p K_T P_T P_H^3}{(1 + K_T P_T + \Sigma K_i P_i)} \cdot a + k_p' P_{but}\, a - k_p' P_{but}. \quad [5]$$

Equation [5] can be written as

$$-(da/dt) = \Psi_s\, a + \Psi_{Rs}\, a - \Psi_{Rs}, \quad [6]$$

where

$$\Psi_s = \frac{k_p K_T P_T P_H^3}{(1 + K_T P_T + \Sigma K_i P_i)} \quad [7]$$

and

$$\Psi_{Rs} = k_p' P_{but}. \quad [8]$$

By defining

$$\Psi_d = \Psi_{Rs} + \Psi_s, \quad [9]$$

Eq. [6] becomes

$$-(da/dt) = \Psi_d (a - \Psi_{Rs}/\Psi_d). \quad [10]$$

Finally, by integrating Eq. [10] for a differential reactor (Ψ_d = constant) the following expression is deduced:

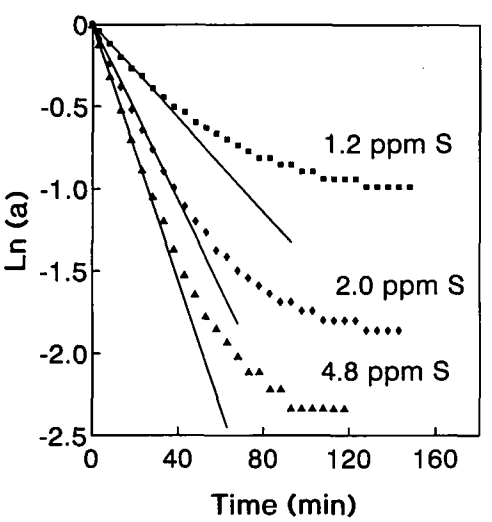

FIG. 2. Experimental results of Fig. 1 represented in a (ln a)-vs-time plot. The values of the slopes at zero time are used for determining TR_E, the experimental catalyst thioresistance.

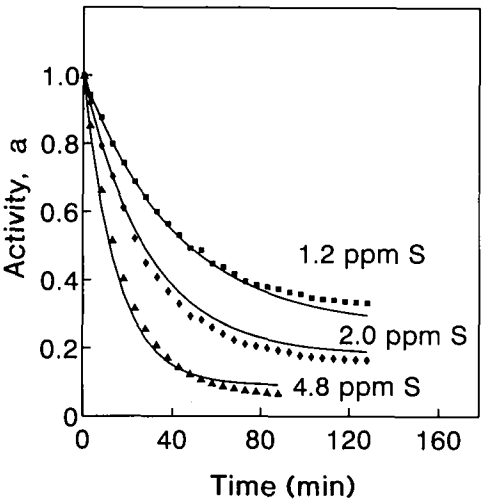

FIG. 3. Time evolution of the activity for the dehydrogenation of cyclohexane, poisoned by thiophene at different concentrations. Catalyst: Pt/Al_2O_3. Points, experimental results; solid lines, model predictions.

$$a = \Psi_{Rs}/\Psi_d + (1 - \Psi_{Rs}/\Psi_d) \cdot \exp(-\Psi_d \cdot t). \quad [11]$$

By taking the limit of Eq. [11] for $t \to \infty$ the residual activity of the catalyst, a_{ss}, is obtained:

$$a_{ss} = \Psi_{Rs}/\Psi_d. \quad [12]$$

In the case of irreversible poisoning, $k_p' = 0$ and so $a_{ss} = 0$ since $\Psi_{Rs} = 0$ according to Eq. [8]; there is not residual activity and Eq. [10] reduces to $-(da/dt) = \Psi_d \cdot a$

Equation [11] was used to compare the DMRA predictions with the experimental results. Parameters Ψ_{Rs} and Ψ_d were obtained by using a nonlinear multivariable least-squares regression which minimizes the objective function $F = \Sigma(a_{exp} - a_{calc})^2$. Figures 3, 4, and 5 compare the activity decay curves obtained for Pt, Pt–Ge, and Pt–Re catalysts, respectively. Similar goodness of fit was obtained with the other catalysts when activities were plotted as a function of time.

III.2 Thiotolerance and thioresistance. The deactivation parameters we have used for determining the relative sensitivity of the catalysts to sulfur poisoning were thiotolerance and thioresistance. Thiotolerance (TT) is defined as the pseudo-steady-state value of the residual activity in the activity decay curves. Obviously, thiotolerance can be employed as a deactivation parameter only when, like in the present case, the deactivation curves reach nonzero steady-state values. According to Eq. [12], the thiotolerance is given by

$$TT = a_{ss} = \Psi_{Rs}/\Psi_d. \quad [13]$$

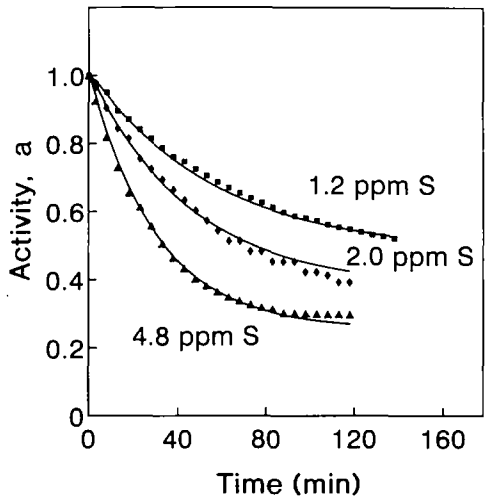

FIG. 4. Time evolution of the activity for the dehydrogenation of cyclohexane, poisoned by thiophene at different concentrations. Catalyst: Pt–Ge/Al_2O_3. Points, experimental results; solid lines, model predictions.

The *TT* values were calculated by using the values of Ψ_{Rs} and Ψ_d obtained from DMRA equations; results for all the catalysts are given in Table 3. For comparison, experimental *TT* values obtained directly as the residual activity values of the activity decay curves were also included in Table 3. A good agreement was observed between experimental values and DMRA predictions. From Table 3 the following thiotolerance order is inferred:

$$\text{Pt–Ge} > \text{Pt–Ir} \cong \text{Pt} \cong \text{Pt–Sn} > \text{Pt–Re}.$$

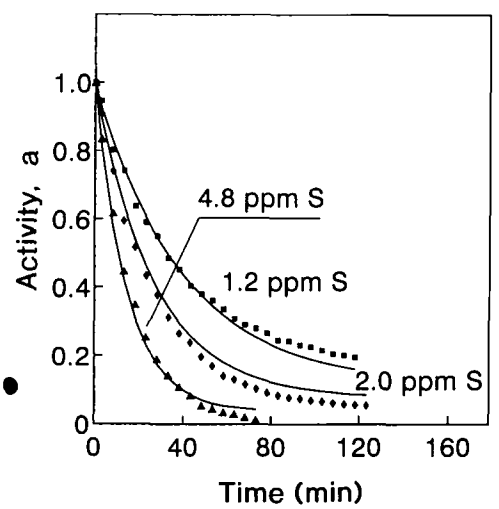

FIG. 5. Time evolution of the activity for the dehydrogenation of cyclohexane, poisoned by thiophene at different concentrations. Catalyst: Pt–Re/Al_2O_3. Points, experimental results; solid lines, model predictions.

The DMRA equations also allowed us to relate thiotolerance with the kinetic parameters describing the poisoning reaction. In fact, from Eq. [7]–[9] and Eq. [13] it is deduced that

$$\frac{1}{TT} = 1 + 1/\left(\frac{P_{but}}{K_p P_H^3} + \frac{1 + \Sigma K_i P_i}{K_p K_T P_H^3} \cdot \frac{P_{but}}{P_T}\right). \quad [14]$$

Equation [14] predicts that for a given thiophene concentration the thiotolerance depends on the thermodynamic equilibrium adsorption constants, K_T and K_p parameters.

Whereas the definition of thiotolerance is widely accepted as the value of the residual activity in the activity decay curves, the concept of thioresistance is not as straightforward. Several parameters like initial deactivation, toxicity, or the intrinsic deactivation constant of pseudohomogeneous kinetics have been used to characterize thioresistance. In this paper we define thioresistance (*TR*) as the inverse of the normalized initial deactivation which can be experimentally estimated from the slope at the intercept of the plots of activity against amount of thiophene fed per exposed metal atom of the fresh catalysts. Thus, thioresistance gives the number of surface metal atoms which are deactivated ab initio of the run by one sulfur atom. Thioresistance is therefore expressed as

$$TR\left[\frac{\text{sulfur atoms}}{\text{surface metal atom}}\right] = \quad [15]$$

$$\frac{1}{(Me_s/F_T) \cdot (-da/dt)_{t\to 0}} = \frac{\beta P_T}{Me_s \cdot (-da/dt)_{t\to 0}},$$

where Me_s = number of surface metal atoms in the catalyst bed, F_T = thiophene flow in the feed (in sulfur atoms/s), and $\beta = NF_v/RT$. Taking the limit of Eq. [10] for $t \to 0$ and replacing in Eq. [15] gives

$$TR = \frac{1}{(\Psi_d - \Psi_{R_s})} \cdot \frac{\beta P_T}{Me_s}. \quad [16]$$

The *TR* values of all the catalysts were calculated by using Eq. [16]. Ψ_d and Ψ_{Rs} were obtained from DMRA equations, and Me_s from the accessible metal fractions given in Table 1. The *TR* values obtained via Eq. [16] are designated TR_R and are summarized in Table 4 for three different thiophene concentrations. Thioresistance was also calculated experimentally (TR_E) by assuming that the initial part of activity decay curves were well represented by an exponential function $a = \exp(-\alpha t)$; then, $-(da/dt)_{t\to 0} = \alpha$ and $TR_E = \beta P_T/Me_s\alpha$. The values of α were determined from the slope of the initial straight line obtained when (ln *a*) was plotted as a function of time as it can be shown in Fig. 2. The TR_E values corresponding

TABLE 3

Catalysts Thiotolerance

Catalyst	1.2 ppm of S		2.0 ppm of S		4.8 ppm of S	
	TT_E[a]	TT_R[b]	TT_E[a]	TT_R[b]	TT_E[a]	TT_R[b]
Pt	0.33	0.26 ± 0.08	0.17	0.18 ± 0.06	0.07	0.09 ± 0.03
Pt–Re	0.18	0.12 ± 0.02	0.04	0.08 ± 0.01	≈0	0.04 ± 0.01
Pt–Ir	0.34	0.24 ± 0.03	0.21	0.16 ± 0.01	0.11	0.08 ± 0.01
Pt–Ge	0.52	0.47 ± 0.01	0.39	0.37 ± 0.01	0.30	0.25 ± 0.01
Pt–Sn	0.37	0.27 ± 0.05	0.16	0.19 ± 0.04	0.09	0.10 ± 0.02

Note. Values determined from experimental curves and from DMRA equations.
[a] Values obtained directly from the experimental deactivation curves.
[b] Values obtained from the deactivation model with residual activity (DMRA).

to all the catalysts are given in Table 4. Both TR_R and TR_E values of Table 4 led to the following thioresistance order:

$$\text{Pt–Ge} > \text{Pt–Ir} \cong \text{Pt} > \text{Pt–Re} > \text{Pt–Sn}.$$

Thioresistance can be related to the kinetic parameters involved in DMRA equations. In fact, from Eqs [16], [9], and [7] it is obtained that

$$TR = \frac{(1 + K_T P_T + \Sigma K_i P_i)}{k_p K_T P_H^3 P_T} \cdot \beta P_T/\mathrm{Me_s} = A + B P_T, \quad [17]$$

where

$$A = \frac{(1 + \Sigma K_i P_i)}{k_p K_T P_H^3} \cdot \beta/\mathrm{Me_s} \quad \text{and} \quad B = \frac{1}{k_p P_H^3} \cdot \beta/\mathrm{Me_s}.$$

According to Eq. [17] the thioresistance is mainly influenced, for a given concentration of thiophene, by the value of k_p, the direct reaction constant of the hydrogenolysis of adsorbed thiophene, and to a lesser degree by K_T, the equilibrium adsorption constant of thiophene. It is significant to note that Eq. [17] predicts that the thioresistance should increase when the thiophene concentration in the feed is increased.

The values of A and B of Eq. [17] were calculated from DMRA equations. The inverse of B is a measure of k_p, the direct kinetic constant of the hydrogenolysis of adsorbed thiophene; in fact $1/B = \text{“}k_p\text{”} = k_p P_H^3 \mathrm{Me_s}/\beta$. By dividing B/A, one obtains $\text{“}K_T\text{”} = B/A = K_T/(1 + \Sigma K_i P_i)$; “$K_T$” is directly proportional to K_T if we accept that $\Sigma K_i P_i$ is almost the same for all the Pt-based catalysts investigated. On the other hand, from Eq. [8] we can obtain $\text{“}k_p'\text{”} = \Psi_{Rs}\beta/\mathrm{Me_s} = k_p' P_{but}\beta/\mathrm{Me_s}$; “$k_p'$” is therefore proportional to k_p', the reverse kinetic constant of the hydrogenolysis of adsorbed thiophene. Finally, by dividing $\text{“}k_p\text{”}/\text{“}k_p'\text{”}$ we obtain $\text{“}K_p\text{”} = \text{“}k_p\text{”}/\text{“}k_p'\text{”} = K_p P_H^3/P_{but}$. The values

TABLE 4

Catalysts Thioresistance

Catalyst	1.2 ppm of S		2.0 ppm of S		4.8 ppm of S	
	TR_E[a]	TR_R[b]	TR_E[a]	TR_R[b]	TR_E[a]	TR_R[b]
Pt	0.92	0.89 ± 0.13	1.00	0.81 ± 0.14	1.14	0.89 ± 0.15
Pt–Re	0.58	0.56 ± 0.11	0.65	0.60 ± 0.12	0.82	0.74 ± 0.14
Pt–Ir	0.97	0.88 ± 0.07	1.06	0.91 ± 0.06	1.16	1.04 ± 0.07
Pt–Ge	1.25	1.15 ± 0.06	1.37	1.25 ± 0.07	1.69	1.49 ± 0.09
Pt–Sn	0.25	0.22 ± 0.04	0.29	0.24 ± 0.04	0.36	0.30 ± 0.05

Note. Values determined from experimental curves and from DMRA equations. *TR* values in atoms of sulfur/surface metal atom. *TR* values of Pt, Pt–Re, and Pt–Ir catalysts were calculated by considering the total metal loading. *TR* values of Pt–Ge and Pt–Sn catalysts were calculated by considering only the Pt loading.
[a] Values obtained directly from the experimental deactivation curves.
[b] Values obtained from the deactivation model with residual activity (DMRA).

TABLE 5

Kinetic and Thermodynamic Parameters of the Poisoning Mechanism Determined from DMRA Equations

Catalyst	"k_p"[a]	"K_p"	"K_T" × 10^9 (atm^{-1})	"K_p" · "K_T" × 10^7 (atm^{-1})
Pt	32.86 ± 0.92	60.38 ± 3.07	3.21 ± 0.42	1.93 ± 0.27
Pt–Re	19.82 ± 0.51	69.18 ± 6.31	7.98 ± 0.86	5.52 ± 0.78
Pt–Ir	20.23 ± 0.28	49.53 ± 0.67	4.98 ± 0.32	2.47 ± 0.16
Pt–Ge	7.42 ± 0.13	19.85 ± 0.40	5.16 ± 0.28	1.02 ± 0.06
Pt–Sn	81.33 ± 3.84	28.40 ± 2.15	6.80 ± 0.77	1.93 ± 0.26

Note. Parameters "k_p," "K_p," and "K_T" are defined in the text.
[a] "k_p" in surface metal atom · atm/sulfur atom.

obtained of "K_T," "K_p," and "k_p" as well as those of product "K_T" · "K_p" are given in Table 5.

DISCUSSION

The relative sensitivity to sulfur poisoning of several naphtha reforming catalysts was established by using two deactivation parameters, namely, thiotolerance and thioresistance, which were determined by developing a deactivation model with residual activity. The experimental deactivation curves were well fitted by the corresponding DMRA curves (Figs. 3–5) and thus the values of both thiotolerance and thioresistance obtained from DMRA equations were similar to those determined directly from the experimental curves (Tables 3 and 4).

Thiotolerance was defined as the value of a_{ss}, the residual activity, and decreased following the sequence Pt–Ge > Pt–Ir ≅ Pt ≅ Pt–Sn > Pt–Re (Table 3). According to Eq. [14], the thiotolerance depends, for a given feed concentration of thiophene, on the values of adsorption equilibrium constants K_p and K_T; the thiotolerance decreases when both K_p and K_T increase. The model allowed us to calculate parameters "K_p" and "K_T" (Table 5) which are in turn proportional to K_p and K_T, respectively. As shown in Table 5, and in agreement with Eq. [14], the values of product "K_p" · "K_T" corresponding to all the catalysts followed an opposite trend compared to the catalyst thiotolerance sequence. The highest "K_p" · "K_T" value (5.52×10^{-7} atm^{-1}) corresponded to bimetallic Pt–Re/Al_2O_3, the least thiotolerant catalyst, and the lowest "K_p" · "K_T" value (1.02×10^{-7} atm^{-1}) was found for Pt–Ge/Al_2O_3 which was the most thiotolerant catalyst. On the other hand, according to the poisoning mechanism the product $K_p \cdot K_T$ is proportional to K_S, the adsorption equilibrium constant of H_2S on the catalyst. In fact, $K_p \cdot K_T = K \cdot K_S$, where $K = P_S P_{but}/P_T P_H^4$ is the global equilibrium constant of the thiophene hydrogenolysis reaction. To confirm this prediction which relates thiotolerance to sulfur adsorption strength, we have measured the amounts of total and irreversibly held sulfur on the catalysts (Table 2). From the inspection of the last column of Table 2 it is apparent that the trend followed by the amounts of sulfur irreversibly held on the catalysts expressed by the S_i/Me_s ratio was the same observed for product "K_p" · "K_T" in Table 5. The general picture emerging from the above results is that catalyst thiotolerance can be qualitatively estimated in a simple way by measuring the amount of irreversibly held sulfur on the catalyst; the higher the S_i/Me_s ratio, the lower the catalyst thiotolerance. To test this interpretation let us examine in greater detail each catalyst.

In the case of Pt–Re/Al_2O_3, as already stated, the adsorption of sulfur on Re is thermodynamically favored compared to Pt and preferentially forms surface Re sulfide (44, 45). Our sulfur adsorption experiments confirmed that Re adsorbs more sulfur than Pt and that sulfur is more strongly bonded to Re than Pt (Table 2, data of sulfur adsorption on Pt/Al_2O_3 and Re/Al_2O_3 samples). This is consistent with the very low thiotolerance exhibited by the Pt–Re catalyst. The Pt–Ir/Al_2O_3 catalyst displayed a thiotolerance similar to that of monometallic Pt catalyst. Thermodynamic calculations and adsorption studies (46, 47) indicate that sulfur bonds more strongly to Ir than Pt. Nevertheless, theoretical calculations predict that the formation of Pt–Ir clusters would occur with Pt surface enrichment since Pt has lower surface energy than Ir (48). The Pt surface enrichment in the formation of Pt–Ir clusters has been corroborated by detailed characterization studies performed on supported Pt–Ir catalysts using Auger electron spectroscopy (49), controlled-atmosphere electron microscopy (50), and X-ray absorption spectroscopy (51). Thus, the formation of a platinum-rich region on the surface of Pt–Ir clusters together with the low amount of Ir contained in the catalyst employed in this study (0.05 wt% of Ir) can account for the similar thiotolerance exhibited for bimetallic Pt–Ir and monometallic Pt catalysts.

The most thiotolerant catalyst was the bimetallic Pt–Ge/Al_2O_3. This is on line with sulfur adsorption experiments which showed that the Ge/Al_2O_3 sample did not adsorb sulfur irreversibly and, a more significant fact, that Ge inhibits the adsorption of irreversible sulfur on Pt in Pt–Ge/Al_2O_3 catalyst (Table 2). Reasons for that are probably due to the formation of bimetallic Pt–Ge clusters. Previous works using X-ray photoelectron spectroscopy (XPS) and temperature-programmed reduction (TPR) techniques (39, 52) have shown that upon H_2 reduction in the 623–773 K range Pt catalyzes the reduction of germanium ions in the immediate surrounding of the metal particles and forms Pt–Ge clusters. Our results using selective chemisorption of H_2, O_2, and CO are consistent with the formation of bimetallic Pt–Ge clusters at relatively low temperature. In fact, after reduction at 573 K, the values of the accessible Pt fractions calculated through HC, OC, and CO were almost the same ($D_{Pt} \cong 50\%$), indicating that the gases were selectively chemisorbed on platinum without any interference from the Ge fraction. However, when reduction was performed at 773 K the values of Pt dispersion were substantially different depending on the gas employed. The apparent value of Pt dispersion diminished drastically when calculated using HC ($D_{Pt} \cong 10\%$) whereas no significant change was observed when oxygen chemisorption was employed ($D_{Pt} \cong 48\%$). These results are consistent with the interpretation that after reduction of the catalyst at 773 K at least a part of Ge cations reduces to metallic Ge and forms bimetallic Pt–Ge clusters. Thus, hydrogen chemisorption decreases because Pt is "diluted" by the Ge atoms which act as an inert and diminish the number of Pt ensembles needed to adsorb hydrogen dissociatively. Bowman and Biloen (52) have investigated the valence state and interaction of Pt and Ge on γ-Al_2O_3 by XPS and they found that Pt is clearly electrodeficient when alloyed with germanium. Goldwasser *et al.* (34), by studying the catalytic properties of the Pt–Ge system in hydrogenation and hydrogenolysis reactions, arrived at a similar conclusion. These authors concluded that the special catalytic properties present in the Pt–Ge system are due to changes in the electronic properties of the platinum, via electron withdrawal by the reduced germanium ions. In an earlier study we have investigated the nature of the S–Pt bond in monometallic Pt/Al_2O_3 catalysts using infrared spectroscopy as characterization technique and CO as probe molecule (28). We found that sulfur acts as an electron-acceptor molecule, decreasing the electronic density of the metal. Consequently, if Pt atoms are electrodeficient in the bimetallic alloyed Pt–Ge particles of the Pt–Ge/Al_2O_3 catalyst, then the strength of sulfur adsorption on Pt should be decreased. This assumption is strengthened by the observation that the amount of sulfur irreversibly adsorbed on the Pt–Ge/Al_2O_3 sample was negligible, thereby explaining the high thiotolerance exhibited by this catalyst.

The Pt–Sn/Al_2O_3 catalyst displayed a thiotolerance similar to that of monometallic Pt/Al_2O_3. Results in Table 2 show that S_i adsorption on Sn/Al_2O_3 sample is negligible and also that the S_i/Pt_s ratio determined for bimetallic Pt–Sn catalyst is similar to that measured for monometallic Pt catalyst. A number of studies have been devoted to the characterization of alumina supported Pt–Sn catalysts. Studies with modern spectroscopy techniques (53) have shown that after reduction at 773 K a part of tin is reduced and forms a metallic Pt–Sn alloy while the other part remains in an oxidized state. Platinum provides the sites for hydrogen activation with subsequent reduction of tin in the vicinity at relatively low temperature. Tin particles which are not in the immediate surrounding of Pt are not subject to this catalytic effect. Thus, the relative amounts of alloyed tin and of Sn(IV) and Sn(II) oxides depend on both the reduction temperature and the atomic Sn/Pt ratio. Regarding the effect of tin on activity, it has been stated that Pt–Sn alloys display very low dehydrogenation activity (54, 55). While our characterization results did not allow us to detect the presence of alloyed tin in the Pt–Sn catalyst, catalytic tests showed that the presence of Sn clearly diminished the activity of Pt in cyclohexane dehydrogenation (Table 1). This result presumably reflects a close interaction between tin and platinum. Whether alloyed or not, our data suggest that the presence of Sn did not diminish to a significant extent the amount of irreversibly held sulfur on platinum and reasonably accounts for the similar thiotolerance Pt–Sn exhibits when compared to monometallic Pt catalyst.

Regarding thioresistance, the TR values determined either from DMRA equations or directly from experimental deactivation curves followed the sequence: Pt–Ge > Pt–Ir ≅ Pt > Pt–Re > Pt–Sn (Table 4). This trend was similar to that established for thiotolerance, excepting for the position of Pt–Sn catalyst which was the least thioresistant catalyst. As shown in Table 4, when the concentration of thiophene in the feed was 1.2 ppm S the first atom of sulfur entering to the reactor deactivated less than one Pt_s atom in the Pt–Ge catalyst, approximately one surface metal atom in both Pt and Pt–Ir catalysts, and between two and four surface metal atoms in Pt–Re and Pt–Sn catalysts, respectively. An interesting prediction is given by Eq. [17]: thioresistance, in contrast to thiotolerance, is increased when the thiophene concentration in the feed is increased; i.e., the number of surface metal atoms initially deactivated by one sulfur atom is decreased when the thiophene concentration in the feed increases. This DMRA prediction is confirmed by the results given in Table 4 that show that the thioresistance systematically increases when P_T increases.

For a given concentration of thiophene, Eq. [16] pre-

dicts that thioresistance depends mainly on the value of k_p, the rate constant of the hydrogenolysis of adsorbed thiophene, and to a lesser degree on the value of K_T, the thiophene adsorption equilibrium constant. The thioresistance is expected to be inversely proportional to k_p; the lower the k_p value, the higher the catalyst thioresistance. From DMRA equations we calculated the values of the parameter "k_p" = $k_p P_H^3 Me_s/\beta$ for all the catalysts (Table 5). From inspection of Table 5 it can be inferred that the trend followed by the inverse of "k_p" is the same we found for catalysts thioresistance. Thus, the lowest value of "k_p" ("k_p" = 7.42 Pt_s atom · atm/S atom) corresponded to bimetallic Pt–Ge catalyst which was the most thioresistant catalyst whereas the highest "k_p" value ("k_p" = 81.33 Pt_s atom · atm/S atom) was found for Pt–Sn catalyst, the least thioresistant catalyst. This correlation between thioresistance and "k_p" is in line with previous studies which attempted to relate sulfur poisoning with hydrodesulfurization (HDS) activity (56, 57). Fréty *et al.* (57) used supported Ir catalysts and studied the effect the support has on sulfur poisoning. They deposited Ir particles on supports of varying acidity and employed the conversion of dibenzothiophene as a measure of HDS activity and the dehydrogenation of cyclohexane doped with thiophene for determining the sulfur sensitivity of the catalysts. In agreement with the present results, they found that the catalysts which displayed higher HDS activity were more deactivated by sulfur poisoning when tested in cyclohexane dehydrogenation.

It should be also noted here that Eq. [17] actually predicts that the thioresistance depends on the intrinsic rate constant $k_p Me_s/\beta$ expressed in (surface metal atom/atom of sulfur · atm^2). This implies that when calculating thioresistance it is necessary to know the number of surface metal atoms of the fresh catalysts. The existence of an accurate method for measuring the metallic dispersion is therefore a prerequisite in determining thioresistance, especially if, as in the present case, catalysts of different chemical composition and metal loadings are employed.

Finally, the metal ratios of catalysts used in this work, measured as Pt/X where X is the second metal, range from 0.53 (Pt–Sn) to 6.30 (Pt–Ir). Because it is known from literature that the atomic metal loading may have strong effects on metallic dispersion as well as on a possible metal–metal or metal–support interaction, care has to be taken for extrapolating these results to other atomic ratios without further work.

CONCLUSIONS

1. Sulfur poisoning of naphtha reforming catalysts was studied by employing cyclohexane as reaction test and thiophene as poisoning molecule. A deactivation model with residual activity was developed to estimate the thiotolerance and the thioresistance of the catalysts. The DMRA model proved to be a useful basis for understanding the effects of various variables of the poisoning mechanism on both thiotolerance and thioresistance.

2. Thiotolerance was in the order Pt–Ge > Pt–Ir ≅ Pt ≅ Pt–Sn > Pt-Re. From DMRA equations and from experimental evidences it was established that the thiotolerance is related to the irreversibly held sulfur on the catalysts: the lower the amount of irreversible sulfur, the higher the thiotolerance.

3. The thioresistance sequence was similar to that determine for catalyst thiotolerance, excepting for the position of Pt–Sn catalyst which was found to be the least thioresistant catalyst. Thioresistance depended mainly on the value of intrinsic hydrogenolysis rate constant of adsorbed thiophene: the lower the rate constant value, the higher the thioresistance.

4. The Pt–Ge catalyst was the most thiotolerant and thioresistant bimetallic catalyst studied. This superior performance is attributed to the formation of Pt–Ge clusters upon H_2 reduction at 773 K that decreases the electronic density of platinum and thereby weakening the strength of the S–P bond.

APPENDIX: NOMENCLATURE

a = activity, defined by $(-r_A)_t/(-r_A)_0$
a_{ss} = residual activity
C_L = concentration of vacant active sites (mol/g)
C_{iL} = concentration of active sites covered by species i (mol/g)
d = deactivation order
F_T = feed rate of thiophene (atoms of sulfur/s)
F_v = volumetric feed rate (cm^3/s)
k_d = deactivation rate constant ($s^{-1} \cdot atm^{-n}$)
k_p = direct reaction constant of the hydrogenolysis of adsorbed thiophene ($s^{-1} \cdot atm^{-3}$)
k'_p = reverse reaction constant of the hydrogenolysis of adsorbed thiophene ($s^{-1} \cdot atm^{-1}$)
K_B = benzene adsorption equilibrium constant (atm^{-1})
K_p = equilibrium constant of the hydrogenolysis of adsorbed thiophene (atm^{-2})
K_T = thiophene adsorption equilibrium constant (atm^{-1})
K_S = H_2S adsorption equilibrium constant
K_I, K_{II} = adsorption equilibrium constants; defined in the cyclohexane dehydrogenation mechanism

L = vacant active sites
L_0 = concentration of active sites of fresh catalysts (mol/g)
Me_s = number of surface metal atoms in the catalyst bed
n = reaction order
N = Avogadro's number (atoms/mol)
$(-r_A)_0$ = reaction rate at zero time (mol of cyclohexane/h · g metal)
$(-r_A)_t$ = reaction rate at time t (mol of cyclohexane/h · g metal)
P_B, P_C, P_H = partial pressure of benzene, cyclohexane, and H_2, respectively (atm)
P_{but}, P_S, P_T = partial pressure of butane, H_2S, and thiophene, respectively (atm)
TR = Thioresistance (sulfur atoms/surface metal atom)
TT = Thiotolerance (dimensionless)
Ψ_d, Ψ_{Rs}, Ψ_s = deactivation functions defined by Eqs. [9], [8], and [7], respectively (s^{-1})

ACKNOWLEDGMENTS

We acknowledge J. Barbier and P. Marecot (Poitiers University, France) for carrying out the sulfur adsorption experiments. We are also grateful to G. McVicker (Exxon Research & Engineering, U.S.A.) for stimulating and helpful discussions. A.M. thanks the Dirección General de Investigación Científica y Técnica, Spain, for financial support.

REFERENCES

1. Hettinger, W. P., Keith, C. D., Gring, J. C., and Teter, T. N., *Ind. Eng. Chem.* **47,** 719 (1955).
2. Minachev, Kh. M., Kondratev, D. A., and Slyunyaev, P. J., *Kinet. Katal.* **2** (5), 690 (1961).
3. Hanner, E., Kaufmann, H., and Leibnitz, E., *Freiberg. Forsch.* **67,** 329 (1964).
4. Jacobson, R. L., Kluksdahl, H. E., McCoy C. S., and Davis R. W., *Proc. Am. Pet. Inst. Div. Ref.* **49,** 504 (1969).
5. Mc Lung, R. G., *in* "Proceedings, 11th Iberoamerican Symposium on Catalysis" (F. Cossio, O. Bermudez, G. del Angel, and R. Gomez, Eds.), Vol. 1, p. 529. Instituto Mexicano del Petróleo, México, 1988.
6. Apesteguía, C. R., and Barbier, J., *J. Catal.* **76,** 352 (1982).
7. Coughlin, R. W., Hasan A., and Kawakami, K., *J. Catal.* **88,** 163 (1984).
8. Dees, M. J., and Ponec, V., *J. Catal.* **115** (2), 347 (1989).
9. Srinivasan, R., and Davis, B. H., *Platinum Met. Rev.* **36** (3), 151 (1992).
10. Barbier, J., Lamy-Pitara, E., Marecot, P., Boitiaux, J. P., Cosyns, J., and Verna, F., *Adv. Catal.* **37,** 279 (1990).
11. Boitiaux, J. P., Cosyns, J., and Verna, F., *in* "Catalyst Deactivation 1987" (B. Delmon and G. F. Froment, Eds.), p. 105. Elsevier, Amsterdam, 1987.
12. Duprez, D., Mendez, M., and Bousquet, J., *Nouv. J. Chim.* **9,** 545 (1985).
13. Maurel, R., and Barbier, J., *J. Chim. Phys.* **11,** 995 (1976).
14. Aguinaga, A., Montes, M., de la Cal, J., and Asua, J. M., *Ind. Eng. Chem. Res.* **31,** 155 (1992).
15. Radovic, L. R. and Vannice, M. A., *Appl. Catal.* **29** (1), 1 (1987).
16. Corella, J., and Monzón, *Ind. Eng. Chem. Res.* **27,** 369 (1988).
17. Fuentes, S., and Figueras, F., *J. Catal.* **54,** 397 (1978).
18. Beeckman, J. W., and Froment, G., *Chem. Eng. Sci.* **35,** 805 (1980).
19. Lynch, D. T., and Emig, G., *Chem. Eng. Sci.* **44** (6), 1275 (1989).
20. Corella, J., and Asua, J. M., *Ind. Eng. Chem. Prod. Res. Dev.* **21,** 551 (1982).
21. Corella, J., Adanez, J., and Monzón, A., *Ind. Eng. Chem. Res.* **27,** 375 (1988).
22. Apesteguía, C. R., Garetto, T. F., and Borgna A., *in* "Catalyst Deactivation 1991" (C. H. Bartholomew and J. B. Butt, Eds.), Vol. 68, p. 399. Elsevier, Amsterdam, 1991.
23. Apesteguía, C. R., and Barbier, J., *Bull. Soc. Chim. Fr.* **5–6,** 1 (1982).
24. Pradier, C. M., Margot, E., Berthier, Y., and Oudar, J., *Appl. Catal.* **43,** 177 (1988).
25. Vassilakis, D., Barbouth, N., and Oudar, J., *Catal. Lett.* **5,** 321 (1990).
26. Apesteguía, C. R., Plaza de los Reyes, J. P., and Garetto, T. F., *Appl. Catal.* **4,** 5 (1982).
27. Apesteguía, C. R., Trevizán, S., Garetto, T. F., Plaza de los Reyes, J. P., and Parera, J. M., *React. Kinet. Catal. Lett.* **20,** (1–2), 1 (1982).
28. Apesteguía, C. R., Brema, C., Garetto, T. F., Borgna A., and Parera, J. M., *J. Catal.* **89,** 52 (1984).
29. Apesteguía, C. R., Garetto, T. F., and Borgna A., *J. Catal.* **106,** 73 (1987).
30. Sinfelt, J. M., Carter, J. L., and Yates, D. J. C., *J. Catal.* **24,** 283 (1972).
31. Eskinazi, V., *Appl. Catal.* **4,** 37 (1982).
32. Bacaud, R., and Figueras, F., *C. R. Acad. Sci. Paris* **281,** 479 (1975).
33. Lieske, H., and Völter, J., *J. Catal.* **90,** 96 (1984).
34. Goldwasser, J., Arenas, B., Bolivar, C., Castro, G., Rodriguez A., Fleitas, A., and Giron J., *J. Catal.* **100,** 75 (1986).
35. De Miguel, S., Martinez Correa, J., Baronetti, G., Castro A., and Scleza, O., *Appl. Catal.* **60,** 47 (1990).
36. Moss, R. L., *in* "Catalysis," Vol. 4, p. 31. The Royal Society of Chemistry, Alden Press, Great Britain, 1981.
37. Palazov, A., Bonev, Ch., Shopov, D., Lietz, G., Sarkany, A., and Völter, J., *J. Catal.* **103,** 249 (1987).
38. De Miguel, S. R., Scelza, A. O., and Castro A. A., *Appl. Catal.* **44,** 23 (1988).
39. Apesteguía, C. R., Garetto, T. F., Brema, C. E., and Parera, J. M., *Appl. Catal.* **10,** 291 (1984).
40. Levenspiel, O., *J. Catal.* **25,** 265 (1972).
41. Fuentes, G., *Appl. Catal.* **15,** 33 (1985).
42. Kehoe, J., and Butt, J., *J. Appl. Chem. Fundam.* **12** (2), 185 (1973).
43. Van Parij, I., and Froment, G., *Ind. Eng. Chem. Prod. Res. Dev.* **25,** 431 (1986).
44. Bartholomew, C., Agrawal, P., and Katzer, J., *Adv. Catal.* **31,** 135 (1982).
45. Biloen, P., Helle J., Verbeek, H., Dautzenberg F., and Sachtler, W. M. H. *J. Catal.* **63,** 112 (1980).
46. McCarty, J., and Wise, H., *J. Catal.* **94,** 543 (1985).
47. Barbier, J., Marecot, P., Tifouti, L., Guénin, M., and Fréty, R., *Appl. Catal.* **19,** 375 (1985).
48. Went, R. C. (Ed.), "Handbook of Chemistry and Physics," 52nd ed. The Chemical Rubber Co., Cleveland, Ohio, 1971.
49. Raser, J. C., Beindorff, W. H., and Scholten, J. J. F., *J. Catal.* **59,** 211 (1979).
50. Baker, R. T. K., Sherwood, R. D., and Dumesic, J. A., *J. Catal.* **66,** 56 (1980).
51. Sinfelt, J., *Sci. Am.* **255** (3), 90 (1985).

52. Bowman, R., and Biloen P., *J. Catal.* **48,** 209 (1977).
53. Verbeek, H., and Sachtler, W. M. H., *J. Catal.* **42,** 257 (1976).
54. Baronetti, G., De Miguel, S., Scelza, O., and Castro, A., *Appl. Catal.* **24,** 109 (1986).
55. Davis, B. H., *in* "New Frontiers on Catalysis" (L. Guczi, F. Solymosi, and P. Tétényi, Eds.), Vol A, p. 889. Elsevier, Amsterdam, 1993.
56. Dhainaut, E., Charcosset, H., Gachet, Ch., and de Mourgues, L., *Appl. Catal.* **2,** 75 (1982).
57. Fréty, R., Da Silva, P., and Guénin, M., *Appl. Catal.* **57,** 99 (1990).